The mechanoelectrical response of the cytoplasmic membrane of *Vibrio cholerae*

Ian Rowe,[1,2] Merina Elahi,[1,3] Anwar Huq,[3] and Sergei Sukharev[1,4]

[1]Department of Biology, [2]Department of Chemistry and Biochemistry, [3]Department of Cell Biology and Molecular Genetics, Maryland Pathogen Institute, and [4]Maryland Biophysics Program, University of Maryland, College Park, MD 20742

Persistence of *Vibrio cholerae* in waters of fluctuating salinity relies on the capacity of this facultative enteric pathogen to adapt to varying osmotic conditions. In an event of osmotic downshift, osmolytes accumulated inside the bacterium can be quickly released through tension-activated channels. With the newly established procedure of giant spheroplast preparation from *V. cholerae*, we performed the first patch-clamp characterization of its cytoplasmic membrane and compared tension-activated currents with those in *Escherichia coli*. Saturating pressure ramps revealed two waves of activation belonging to the ∼1-nS mechanosensitive channel of small conductance (MscS)-like channels and ∼3-nS mechanosensitive channel of large conductance (MscL)-like channels, with a pressure midpoint ratio $p_{0.5}$MscS/$p_{0.5}$MscL of 0.48. We found that MscL-like channels in *V. cholerae* present at a density three times higher than in *E. coli*, and yet, these vibrios were less tolerant to large osmotic downshocks. The *Vibrio* MscS-like channels exhibit characteristic inward rectification and subconductive states at depolarizing voltages; they also adapt and inactivate at subsaturating tensions and recover within 2 s upon tension release, just like *E. coli* MscS. Trehalose, a compatible internal osmolyte accumulated under hypertonic conditions, significantly shifts activation curves of both MscL- and MscS-like channels toward higher tensions, yet does not freely partition into the channel pore. Direct electrophysiology of *V. cholerae* offers new avenues for the in situ analysis of membrane components critical for osmotic survival and electrogenic transport in this pathogen.

The Journal of General Physiology

INTRODUCTION

Strong osmotic forces constantly affect all microorganisms, probably with only a few exceptions of obligatory symbionts or parasites. A cell 2 µm in diameter, surrounded by a single unarmored membrane, would burst with only a 20-mosmol inside versus outside osmotic gradient. At the same time, most gram-negative bacteria survive 600–1,000-mosmol downshocks with uncompromised viability (Britten and McClure, 1962; Csonka and Hanson, 1991; Schleyer et al., 1993; Wood et al., 2001). The early perception was that bacteria can tolerate high internal pressure because they are surrounded by a rigid cell wall, but the peptidoglycan network was shown to be stretchable (Koch and Woeste, 1992), and the more common opinion now is that the bacterium survives mostly because of its ability to rapidly dissipate excess osmolytes through a special emergency release system (Martinac et al., 1987; Levina et al., 1999). This system consists of several types of mechanosensitive channels activated at different tension thresholds (Berrier et al., 1996; Schumann et al., 2010; Naismith and Booth, 2012), with mechanosensitive channel of small conductance (MscS) and mechanosensitive channel of large conductance (MscL) mediating the bulk of osmolyte release. The success of the rescuing operation depends on one simple condition: the release of excess osmolytes must outpace the rate at which the lytic level of hydrostatic pressure inside the cell is reached. It is not surprising that expression of mechanosensitive channels is under the control of transcription factors regulating stress responses (Stokes et al., 2003), especially responses to cell wall damage. It is now obvious that bacterial mechanosensitive channels are capable of quickly dissipating ionic gradients (Boer et al., 2011), but their permeabilities to organic compatible osmolytes have not been studied. Functional properties of such channels are under intense scrutiny through the application of direct electrical recording (Martinac et al., 1987), reconstitution (Sukharev et al., 1993), and structural (Perozo, 2006; Steinbacher et al., 2007) and computational (Gullingsrud and Schulten, 2003; Anishkin et al., 2008) techniques, but limited primarily to *Escherichia coli*.

Facultative pathogens that spend part of their life as free-living forms face the same problem of osmotic adaptation. *Vibrio cholerae* populates an extremely broad range of aquatic environments, from rain water to deep

Correspondence to Sergei Sukharev: sukharev@umd.edu

Abbreviations used in this paper: LB, Luria-Bertani medium; MscL, mechanosensitive channel of large conductance; MscS, mechanosensitive channel of small conductance.

The Rockefeller University Press $30.00
J. Gen. Physiol. Vol. 142 No. 1 75–85
www.jgp.org/cgi/doi/10.1085/jgp.201310985

sea water of high salinity (Pruzzo and Huq, 2005; Grim et al., 2010; Huq and Grim, 2011) and estuarial zones, where the salinity and osmotic pressure can broadly fluctuate. Pathogenic strains of *V. cholerae* are transmitted predominantly through fresh water, in which it is typically dropped from the intestines (Barcina, 1995). The fact that microorganisms survive these abrupt changes in osmolarity implies a very efficient osmoregulation system (Keymer et al., 2007; Naughton et al., 2009) that enhances environmental stability and transmission from one host to another. Extension of the electrophysiological platform to *V. cholerae* may uncover new aspects of its osmoregulation system that are critical for osmotic survival. Previously, biophysical properties of the outer membrane channels (porins) from *V. cholerae* were studied in reconstituted systems (Duret and Delcour, 2006; Duret et al., 2007; Pagel and Delcour, 2011), with the emphasis on adaptation to the intestinal environment. The membrane aspects of *V. cholerae* osmotic survival in fresh water have not been studied in direct electrophysiological experiments before.

Here, we adapted the giant spheroplast preparation technique to *V. cholerae*, previously developed for *E. coli*, and completed the first patch-clamp survey of its cytoplasmic membrane. We found two dominant channel activities similar to MscS and MscL in *E. coli*. Despite a higher overall density of mechanosensitive channels, *V. cholerae* exhibits lower tolerance to large osmotic shocks. We present the first comparison of channel activities between the two enteric species, emphasizing differences that suggest parameters that may define environmental fitness of these bacteria.

MATERIALS AND METHODS

Strains, spheroplast preparation, and electrophysiology

WT *V. cholerae* (N16691) from A. Huq's laboratory and WT *E. coli* strain AW405, provided by J. Adler (University of Wisconsin, Madison, WI), were used in the study. The original procedure of giant spheroplast preparation from *E. coli* (Ruthe and Adler, 1985; Martinac et al., 1987) includes a 1.5–2-h incubation in the presence of 0.06 mg/ml cephalexin, during which bacteria produce long filamentous cells. The filaments are resuspended in 1 M sucrose buffer and subjected to lysozyme digestion (0.2 mg/ml) in the presence of 5 mM EDTA. Within 5–10 min of lysozyme treatment, filaments collapse into spheres of 3–6 µm in diameter, at which point the reaction is stopped with excess Mg^{2+}. Spheroplasts are separated from the rest of the reaction and debris using quick sedimentation through a one-step sucrose gradient. Spheroplasts were stored in a high sucrose/BSA medium at −80°C. This procedure was used to make AW405 *E. coli* spheroplasts and was applied to N16961 *V. cholerae* with adaptations as described in Results.

Borosilicate glass (Drummond) was empirically shown to be suitable for tight-seal formation with bacterial membranes. Channel activities in giant spheroplasts were recorded from excised membrane patches at voltages between −80 and 80 mV. Negative pressures (suction) were applied to patches with a high speed pressure-clamp apparatus (HSPC-1; ALA Scientific Instruments). Pressure protocol programming, data acquisition, and analysis were performed using PClamp 10 software (Molecular Devices). Ensemble and single-channel currents were analyzed after Rs correction of the traces by the equation, $G_P = I/(V - IR_S)$, where G_P is the patch conductance and V and I are the transmembrane voltage and current, respectively. The series pipette resistance ($R_S \approx 2.5$–3 MΩ) was determined in each experiment after the patch broke.

To analyze the effect of trehalose on single-channel conductance, we used the macroscopic equation accounting for the pore (R_p) and access (R_s) resistances separately: $R_{ch} = R_p + R_s = (l + 0.5\pi a)\rho/\pi a^2$, where l and a are the length and radius of the pore (Hall, 1975; Hille, 2001). Specific resistances (ρ) of recording buffers with and without trehalose were measured using CDM230 conductivity meter (Radiometer).

The midpoint of activation was determined with 1-s saturating pressure ramp protocols, and the change in midpoint was monitored before and after the addition of trehalose to the bath. A combination of ramps of varying duration was used to visualize single-channel events to determine the current passing through a single channel. Inactivation of the MscS-like channel was examined with protocols that compared the number of channels available both before and after the patch was held under a subsaturating tension for 10 s. Specific protocols are explained in the figure legends.

Osmotic survival experiments

After observing large tension-activated conductances and anticipating corresponding osmotic permeability responses, we compared osmotic shock survival for *V. cholerae* and *E. coli*, in parallel side-by-side experiments. Both species grow well in Luria-Bertani medium (LB) plus 3% NaCl (HiLB, 1,180 mosmol). Fresh overnight cultures were diluted at 1:100 in this medium and pregrown for 2 h to OD600 of ∼0.4. The high osmolarity–adapted cultures (50-µl aliquots) were then abruptly shocked into 5 ml of diluted media (LB, LB/2, LB/4, LB/8, LB/16, and distilled water). After a 15-min incubation and quick 1:200 dilution in the medium it was shocked, each culture was plated in duplicates, and the

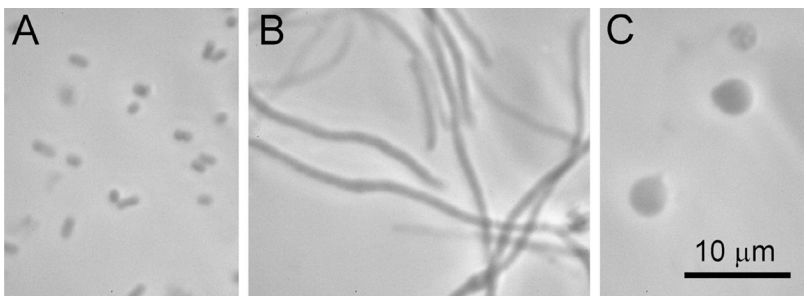

Figure 1. Phase-contrast images of the intact *V. cholerae* cells (A), cephalexin-induced filaments (B), and giant spheroplasts after a 20-min incubation with EDTA and lysozyme (C).

colonies were counted the next morning. Osmolarities of media were measured using a vapor pressure osmometer (5520; Wescor Biomedical Systems).

RESULTS

Vibrio spheroplast preparation

The original procedure of giant spheroplast preparation from *E. coli* (Ruthe and Adler, 1985) was adapted by Martinac et al. (1987) for patch clamp; it includes a 1.5–2-h incubation in the presence of 0.06 mg/ml of the septation blocker cephalexin, during which bacteria grow but do not divide, producing filamentous cells. Our results show that *V. cholerae* is susceptible to both cephalexin and lysozyme. Filamentous forms grew in LB broth in the presence of 0.1 mg/ml cephalexin at the approximate rate of 100 μm/h. Filaments 80–150-μm long remained stable after sedimentation at 2,000 *g* and gentle pipetting. The concentration of lysozyme (0.4 mg/ml) and EDTA (25 mM) required for spheroplast formation in *V. cholerae* was twice what was needed for analogous *E. coli* preparations and on average took 20–30 min, which is also double the requirement of *E. coli*. Spheroplasts were separated from the debris by centrifugation through 1 M sucrose. Fig. 1 illustrates relative sizes of intact bacteria, filamentous forms, and giant spheroplasts. Spheroplasts often had a slightly irregular nonspherical shape, signifying remnants of undigested peptidoglycan.

Mechanoelectrical responses of the inner membrane to pressure ramps

Under sustained 20–40-mm Hg suction delivered from the pressure-clamp apparatus, *V. cholerae* spheroplasts formed tight seals with borosilicate glass pipettes, typically within 2–15 min. As with *E. coli*, patch excision was achieved by tapping on the base of the micromanipulator. Inside-out patches stimulated by triangular ramps of saturating pressure under a 30-mV hyperpolarizing voltage exhibited 2–7-nA currents in both types of preparations, which invariably displayed two-wave responses (Fig. 2 A). In *E. coli*, the first wave was ascribed to the MscS population, possibly with a mixture of a few MscK channels (Li et al., 2002), and the second, activating at higher tensions, represents a uniform MscL population. In *V. cholerae*, we observed very similar two-wave responses, usually with a lesser relative amplitude of the first wave. Relative amplitudes of the two waves were essentially independent on the speed of the pressure ramp. To avoid voltage-clamp errors caused by pipette series resistance (Rs) under high (>2-nA) currents, Rs correction was introduced (see Materials and methods). The corrected traces provided fractions of the total conductance ascribed to each type of channel and pressure midpoints for activation. The ramp responses clearly show that in both enteric bacteria, MscL is the dominant conductance responsible for the bulk of tension-activated permeability increase. MscS-like channels in *Vibrio* represent a considerably smaller fraction

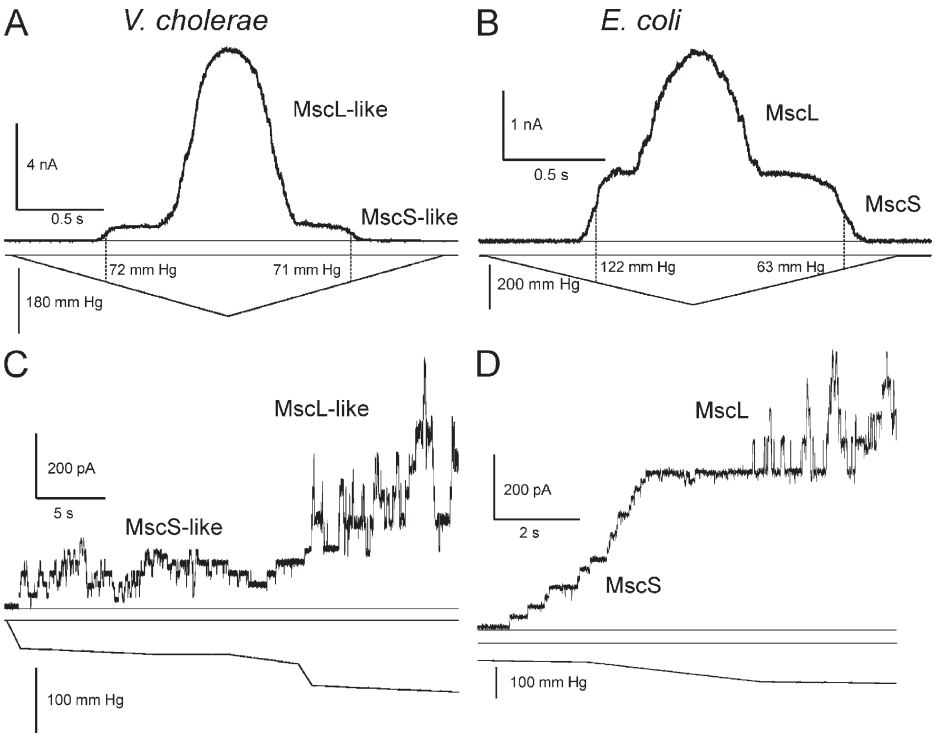

Figure 2. Mechanoelectrical responses of *V. cholerae* and *E. coli* membrane to ramps of pressure. (Top) Typical response of an excised inside-out patch to a 1-s saturating triangular ramp in *V. cholerae* (A) and *E. coli* (B). Responses of the same patches to a slow nonsaturating ramp protocol designed to reveal single-channel conductances for *V. cholerae* (C) and *E. coli* (D).

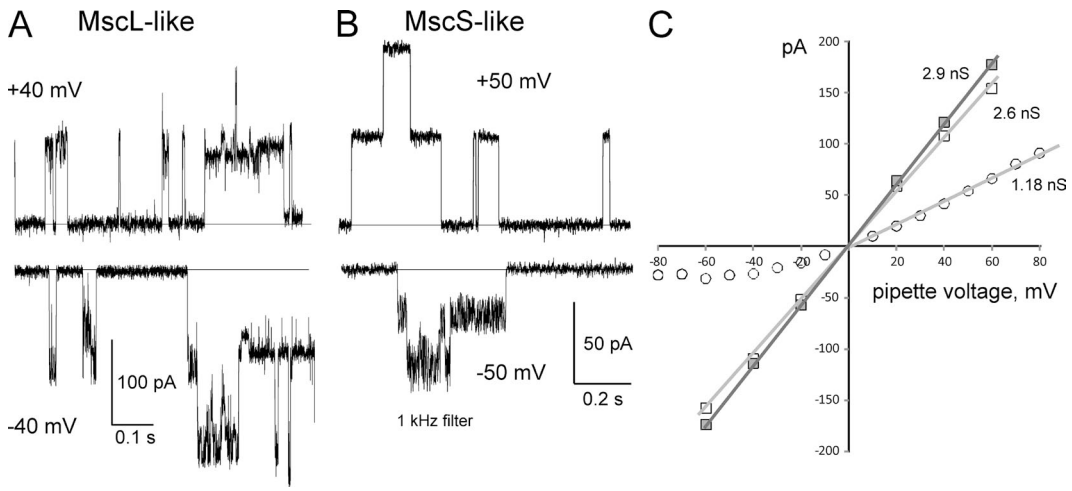

Figure 3. I-V relationships for the two dominant channel conductances in *V. cholerae*. (A and B) Examples of single-channel currents at opposite voltages for both the MscL-like and MscS-like channels. Note fast-flickering subconductance levels in MscS at negative pipette potentials. (C) I-V plot of MscL-like (squares) and MscS-like channels (circles). Filled squares represent the Rs-corrected curve for MscL. MscS shows obvious inward rectification.

of conductance compared with MscS of *E. coli*; they also show no activation hysteresis (difference in midpoints on the ascending and descending legs of the triangular ramp), whereas half of *E. coli* MscS deactivates at a considerably lower pressure compared with the activation midpoint, producing an asymmetrical ramp response (Fig. 2 B).

To determine unitary conductances, we applied sequences of slower ramps to visualize single-channel events (Fig. 2, C and D). From multiple traces taken at different voltages, we created I-V plots and determined slope conductances at hyperpolarizing voltages (pipette positive) for single MscS-like (1.0 ± 0.1 nS) and MscL-like channels (2.6 ± 0.1 nS, or 2.9 nS after Rs correction) of *V. cholerae* (Fig. 3). This information permitted us to quantify the numbers and densities of channels in each preparation. Based on the previous results that the pressure midpoints for *E. coli* MscL correspond to ~12-mN/m tension (Sukharev et al., 1999; Moe and Blount, 2005), we estimated the radius of curvature and area for each *E. coli* patch using the law of Laplace. Because we used the same 2.5–3-MOhm pipettes throughout this project, we first assumed that the average geometry of patches in both preparations was the same. The second assumption was that the tension midpoints for *E. coli* MscL and *V. cholerae* MscL-like channels are the same (Moe et al., 1998). Using these two different assumptions, we estimated patch areas and densities of channels in each preparation. The first assumption (Table 1, columns 4 and 5) gave a 20% lower estimation of channel density in *V. cholerae* relative to the second assumption (columns 8 and 9) because of a slight difference in estimated mean patch radius (1.37 vs. 1.50 μm).

The comparison of the ensemble currents in multiple patches (Fig. 1) reveals modest but statistically significant differences in activation midpoint ratios and substantial differences between channel numbers and densities in the membranes of *E. coli* and *V. cholerae* (Table 1). In *E. coli* (AW405), MscS and MscL are present on average at 3.6 and 4.3 channels/μm^2, with a ratio of midpoint pressures of 0.60 ($p_{0.5}$MscS/$p_{0.5}$MscL). The MscS-like and MscL-like channels occur in *V. cholerae*

TABLE 1

Experimental occurrences of MscS-like and MscL-like channels in patches of WT E. coli and V. cholerae

Species	1	2	3	4	5	6	7	8	9
	No. MscS per patch	No. MscL per patch	$p0.5_{MscS}/p0.5_{MscL}$	MscS/μm^2 (r = 1.5 μm)	MscL/μm^2 (r = 1.5 μm)	Patch r*, μm (γ0.5 = 12 mN/m)	Patch area*, μm^2	MscS/μm^2*	MscL/μm^2*
E coli	46 ± 14	61 ± 40	0.60 ± 0.05	3.6 ± 1.8	4.3 ± 2.2	1.5 ± 0.3	14.7 ± 5	3.6 ± 1.8	4.3 ± 2.2
V cholerae	17 ± 9	164 ± 100	0.48 ± 0.04	1.2 ± 0.7	11 ± 4	1.37 ± 0.3	12.4 ± 6.3	1.5 ± 0.8	14 ± 5

Multiple traces, as shown in Fig. 2, were Rs corrected, and numbers of MscS-like and MscL-like channels as well as midpoint pressures for each population were determined. The pressure midpoint ($p_{0.5}$) for Eco MscL was equated to membrane tension $\gamma_{0.5}$ = 12 mN/m acting on channels, from where the radii of patch curvature and areas were calculated according to the law of Laplace ($\gamma = \Delta pr/2$). The densities (channels/μm^2) were then deduced for MscS-like and MscL-like channels individually, first on the assumption that the average patch radius for *V. cholerae* preparations is the same as for *E. coli* (columns 4 and 5) and independently with the assumption that MscLs in both preparations gate with the same midpoint γ0.5 = 12 mN/m (columns 6 through 9). Data are presented as mean ± SD (n = 12 for *E. coli* and n = 19 for *V. cholerae*). The midpoint ratios $p0.5_{MscS}/p0.5_{MscL}$ for the two species (column 3) are significantly different at a 0.006 level according to two-tailed unequal variance t test.

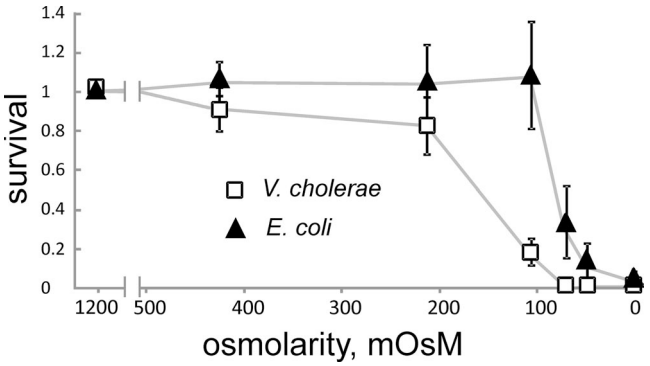

Figure 4. Viability of *V. cholerae* and *E. coli* upon osmotic downshifts of different magnitude. Both cultures were pregrown at 1,180 mosmol (LB containing 0.52 M NaCl) for 2 h and then abruptly diluted into media of different osmolarity as indicated on the horizontal axis. After 15 min of incubation, the cultures were further diluted and plated in duplicates. The survival is expressed as the number of colonies relative to the unshocked control. The data points are averages of six independent experiments, with error bars representing standard deviation.

(N16961) at densities of 1.2 and 11 channels/μm^2, respectively, with a midpoint ratio of 0.48. Based on the data shown in Fig. 2 and Table 1, MscL-like channels are present at a 2.5 times higher density and MscS-like channels are present at a third the density in *V. cholerae* compared with *E. coli*. These differences in channels densities, confirmed in three independent batches of spheroplasts, prompted us to compare resistances of the two strains against acute osmotic downshock. The inference was that the higher overall density of channels in *V. cholerae* should correlate with higher osmotic survival.

Osmotic survival of *V. cholerae*

Survival rates of estuarial/enteric *V. cholerae* were quantified with that of primarily enteric *E. coli* in parallel osmotic dilution and plating experiments. Both cultures were pre-adapted in high osmotic LB (LB base with 0.52 M NaCl and 1,180 mosmol), where they grew for 2 h to OD_{600} of ~0.5. The cultures were then abruptly diluted at 1:100 into media of different osmolarity (1,180, 425, 212, 106, 70, and 48 mosmol and distilled water). As seen from Fig. 4, both cultures easily survived a 970-mosmol downshift, after which the number of colonies for *V. cholerae* decreased. *E. coli* remained completely viable after an ~1,100-mosmol drop, but beyond that point its survival precipitously declined as well. Remarkably, between the final osmolarity of 48 mosmol (LB/16) and distilled water, there was almost no difference in the survival rates: ~2–4% *E. coli* and ~0.3–0.1% *V. cholerae*. Although osmotic shock tolerance is comparable in the two enteric species, *V. cholerae* is clearly more sensitive despite the fact that it had the overall higher density of mechanosensitive channels. We hypothesize that this higher density of mechanosensitive channels may be a compensation for some other vulnerable traits of *Vibrio*, such as cell geometry, elasticity of

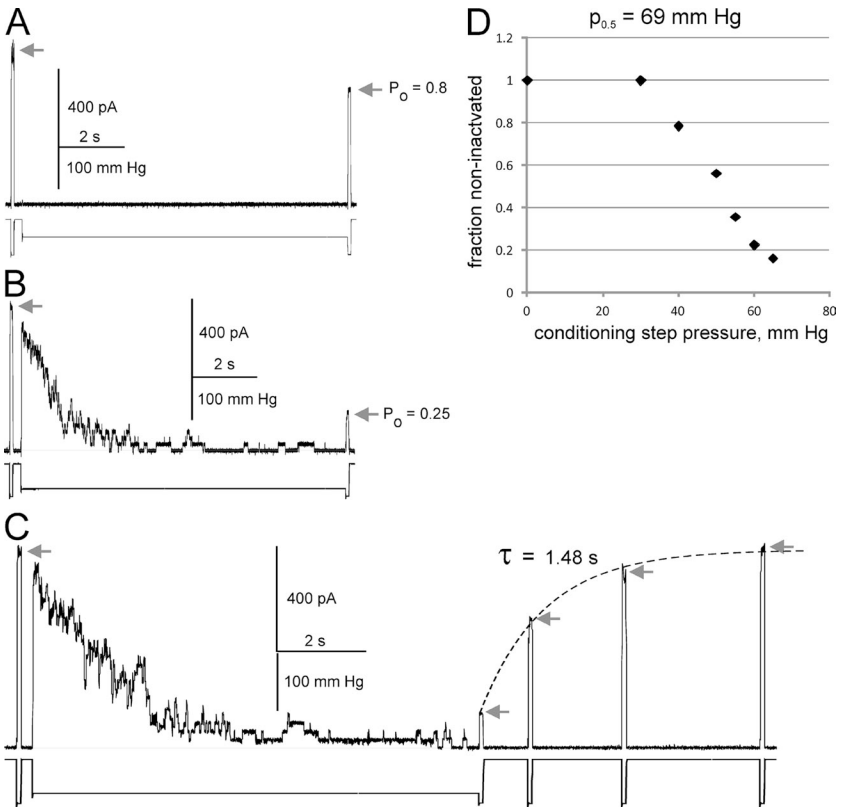

Figure 5. Inactivation and recovery of the *Vibrio* MscS-like channel. (A) Patch response to the pulse-step-pulse protocol with a subthreshold step amplitude. Saturating pulses before and after the step reveal the initial and remaining active population. (B) A similar experiment with activation of nearly the entire population during the step. (C) The recovery experiment. Fitting of the tips of the test pulse responses reveals τ recovery of 1.5 ± 0.2 (n = 3) s. (D) Dependence of the noninactivated fraction of MscS-like channels on the amplitude of intermediate pressure step illustrates that inactivation is tension driven.

the cell wall, or limited permeability of channels to specific osmolytes. The possible reasons for *Vibrio* vulnerability are presented in Discussion. The repeated observation of surviving colonies in distilled water suggests that bacterial populations are nonuniform and always contain a small fraction of highly resistant cells.

I-V relationships for the two dominant activities

To investigate how closely mechanosensitive channel activities in *V. cholerae* resemble those in *E. coli*, we measured I-V curves in a broad range for the two dominant activities. It was easier to record single MscS-like channels, which activate at a relatively low threshold, when the patch was initially silent. Conversely, to characterize MscL-like activities, we had to saturate the population of MscS-like channels first and record single MscL-like activities on top of a 1-nA current plateau. Because of reduced patch resistance in the presence of 8–10 open MscS-like channels, the MscL-like channels conducted at apparent 2.6 nS. After Rs correction (Rs = 2.9 MΩ, the open pipette resistance), the conductance was close to the 3.0-nS activity reported for MscL channels recorded in MscS-null *E. coli* strains (Levina et al., 1999; Chiang et al., 2004). In parallel experiments, *E. coli* MscL exhibited an apparent conductance of 2.4 nS when recorded at the background of ∼20 saturated MscS channels, 22% lower than the previously established unitary conductance of *E. coli* MscL. We also observed that the large-conductance channel from *Vibrio* also had a stronger propensity toward the uppermost subconductive state than *E. coli* MscL (compare Fig. 3, A and B).

The *Vibrio* MscS-like channel displayed a substantial inward rectification; the I-V curves were linear at hyperpolarizing voltages (pipette positive) but had a lower slope at depolarizing voltages. This MscS-like channel exhibited open-state noise at depolarizing (negative pipette) voltages, similar to what was observed in *E. coli* MscS (Akitake et al., 2005). These fast-flickering substates are likely to be the reason for rectification.

MscS-like channel inactivates and recovers

The earlier saturation of MscS-like channel population (plateau in Fig. 2 A) allowed us to choose a pressure range at which we could see activity only from this channel. Traces presented in Fig. 5 show patch responses to a pulse-step-pulse protocol, revealing the processes of adaptation and inactivation. In each protocol, the first short saturating pulse applied in the beginning revealed the entire active population, whereas the next prolonged step of pressure conditions the process of inactivation. The short saturating pulse delivered at the end tests for the remaining active population. The trace presented in Fig. 5 A shows a noticeable inactivation under a subthreshold step that did not invoke any activity. When the conditioning pressure step was at the midpoint for channel activation (determined with a 1-s ramp), inactivation was maximal (Fig. 5 B). The recovery experiment (Fig. 5 C) used a similar protocol; after the conditioning step pressure was dropped to zero, the patch was probed by a sequence of saturating pulses, tracing the process of recovery from inactivation. As illustrated in Fig. 5 D, inactivation of the MscS-like

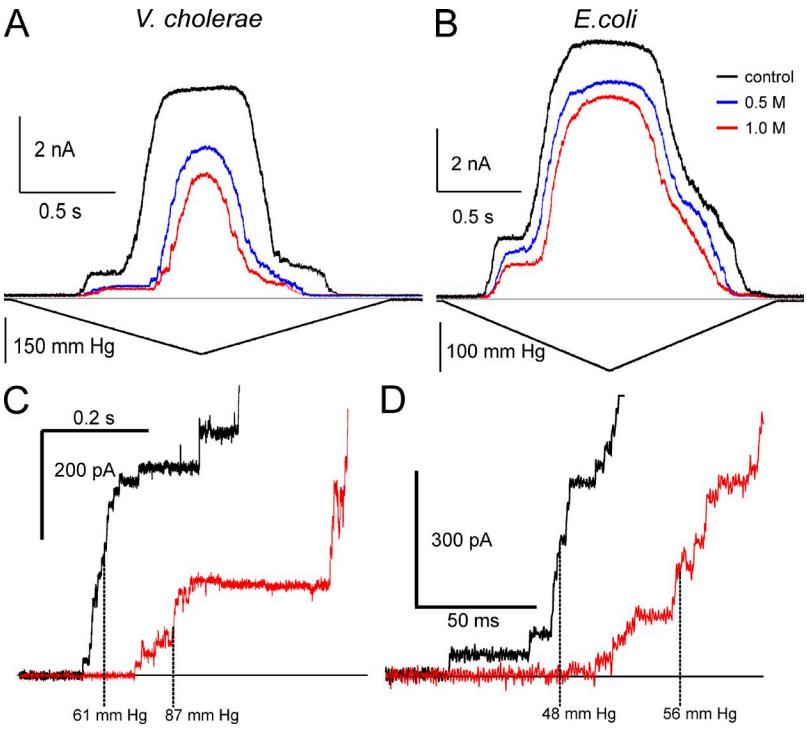

Figure 6. Effects of trehalose on MscS-like and MscL-like channel activation. Trehalose induces substantial left-shift of activation curves, which is more pronounced for MscL in *V. cholerae* (A) than in *E. coli* (B). The three curves represent trehalose concentrations of 0 (black), 0.5 (blue), and 1.0 M (red). Magnified early responses in *V. cholerae* (C) and *E. coli* (D) specifically show the right-shift of the MscS curve as well as reduced single-channel conductance in response to 1 M trehalose.

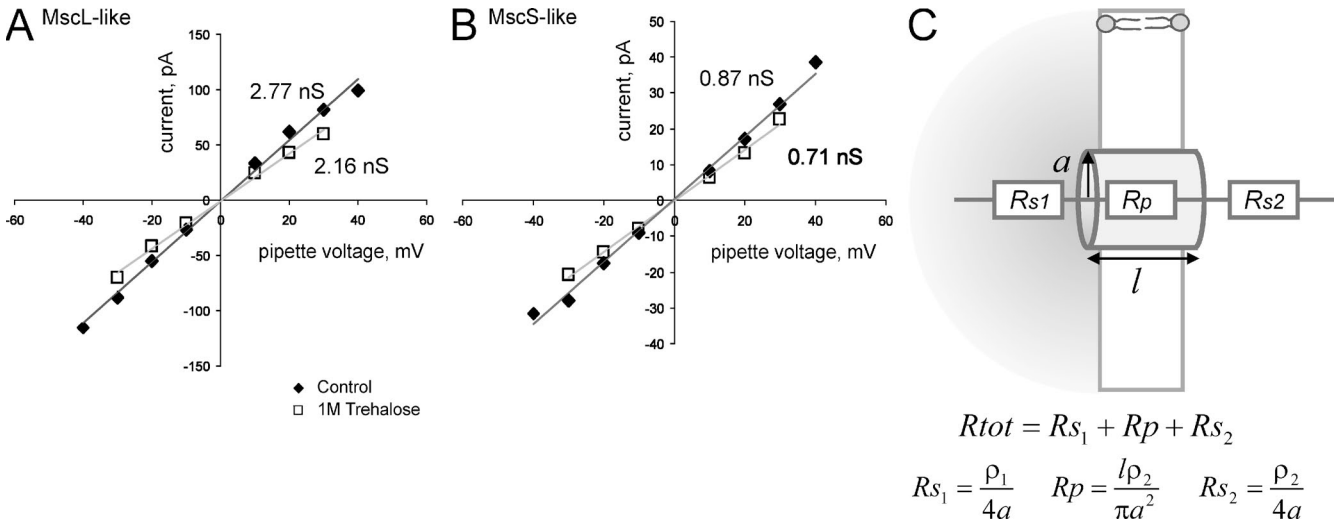

Figure 7. I-V relationships for single-channel currents recorded in control and in the presence of 1 M trehalose on the cytoplasmic side for MscL-like and MscS-like channels in *V. cholerae*. (A and B) Each plot presents the data of one typical experiment, with all I-V curves obtained on the same patch. The unilateral addition of trehalose decreased the slope conductance by a factor of 0.78 ± 0.03 for MscL-like and by a factor of 0.80 ± 0.06 for MscS-like channels (mean ± SD; $n = 4$; based on four independent experiments). (C) Model of a channel, depicting how the total series resistance (R*tot*) is determined by the pore itself (*Rp*) as well as the access resistance on either side of the membrane (Rs_1 and Rs_2). The values are dependent on channel radius (a), length (l), and the conductivity of the solution (ρ), which can be found in Table 2. Shaded area on the left represents the compartment with trehalose.

channel is tension driven. The *Vibrio* MscS-like channel thus behaved very much like *E. coli* MscS (Akitake et al., 2005; Kamaraju et al., 2011), with one subtle difference: it shows a small amount of silent inactivation at tensions that invoke no activity (Fig. 5 A).

Both MscS-like and MscL-like channels are modulated by compatible osmolytes

Ramp responses of the entire channel population in control and in the presence of 0.5 or 1 M trehalose on the cytoplasmic side of the patch are demonstrated in Fig. 6. *V. cholerae* (Fig. 6 A) and *E. coli* (Fig. 6 B) are both shown to be sensitive to the presence of this compatible osmolyte, evident by a right-shift of the activation curve and a decrease of the active population. The bottom panels (Fig. 6, C and D) show the magnified responses of MscS-like channels at the foot of the trace in both control and with 1 M trehalose traces. In four independent experiments, the average shift of MscS activation midpoint in the presence of 1 M trehalose was 24 ± 16% for *V. cholerae* and 12 ± 5% for *E. coli*. Shifts of MscL-like channels were 24 ± 4% and 11 ± 2% for *V. cholerae* and *E. coli*, respectively. It is clear that trehalose modulates channel activity, possibly through tension-driven intercalation into the bilayer (Rudolph et al., 1986; Luzardo et al., 2000; Villarreal et al., 2004) or perhaps through an osmotic or crowding effect, which has been shown to promote MscS inactivation (Grajkowski et al., 2005). We have also observed right-shifts of MscL-like channel activation in the presence of 1 M glycine-betaine, another compatible osmolyte. Glycine-betaine exerted no visible effect on the MscS-like channel of *Vibrio*.

I-V relationships were analyzed for the two dominant channel activities in the absence and presence of trehalose on the cytoplasmic side of the patch. Fig. 7 shows these changes upon the addition of 1 M trehalose. Data (Fig. 7 and Table 2) were treated using the macroscopic conductance equation (Hille, 2001), which accounts for pore resistance (*Rp*) and access resistances from each side of the channel (Rs_1 and Rs_2) (see Materials and methods and Fig. 7 C). Previously, it was shown that the unitary conductances of both MscL and MscS scale

TABLE 2

Parameters for V. cholerae channels fitted with the macroscopic conductance equation

Channel	Parameters	Gexp	ρ1	ρ2	ρ3	Gcalc
	nm	*nS*	*Ωcm*	*Ωcm*	*Ωcm*	*nS*
MscL-like	$l = 4.6$, $r = 1.44$	control 2.75	33.3	33.3	33.3	2.75
		+ trehalose 2.15	98	33.3	33.3	2.16
MscS-like	$l = 5.4$, $r = 0.8$	control 0.87	33.3	33.3	33.3	0.87
		+ trehalose 0.71	98	37.0	33.3	0.71

Hall, 1975; Hille, 2001.

linearly with specific conductivity of the recording buffer, suggesting bulk-like conditions for ion transport through wide water-filled pores (Sukharev et al., 1999; Sukharev, 2002). Conductivity measurements indicated that specific resistance of the recording buffer increased three times, from 33 to 98 Ωcm in the presence of 1 M trehalose. We presumed, if trehalose freely partitioned into the channel pore, that we would observe a proportional decrease in pore conductance. Values of conductance determined from the data (G_{exp}) match closely with those calculated via the macroscopic conductance equation (G_{calc}); variation of only Rs_1 (the cytoplasmic side of the membrane patch) proportional to changes of bulk-specific resistance (ρ) caused by trehalose sufficiently explains the observed change in unitary currents. This suggests that the resistance of the pore itself (R_p) does not visibly change upon osmolyte addition, and thus, trehalose does not freely partition from the cytoplasm or accumulate in MscS-like or MscL-like pores. Prefilters on the cytoplasmic side of each channel formed by C-terminal domains (Chang et al., 1998; Anishkin et al., 2003; Steinbacher et al., 2007) may impede partitioning, whereas the exit toward the periplasm is likely to be unimpeded. The presented data do not exclude trehalose permeation through MscL or MscS pores; it simply shows that the steady-state pore occupancy with the osmolyte is low, possibly because of a slower (prefilter-limited) entry rate from the cytoplasmic side and a higher rate of exit on the periplasmic side.

DISCUSSION

V. cholerae readily produces filamentous forms and giant spheroplasts under experimental conditions similar to what was developed for *E. coli*. This enables direct patch-clamp characterization of the *V. cholerae* cytoplasmic membrane and the individual components involved in osmotolerance. The first electrophysiological survey of *V. cholerae* revealed a robust tension-stimulated conductance response mediated by two dominant types of mechanosensitive channel activities, similar to what was observed in *E. coli*: the MscS-like (0.8–1-nS) and MscL-like (2.6–3-nS) channels. The N16961 *V. cholerae* genome (Heidelberg et al., 2000) harbors one clear orthologue of *E. coli* MscL (available at RefSeq under accession no. NP_233001; 136 amino acids [aa], 65% identity) and a likely orthologue of *E. coli* MscS (available at RefSeq under accession no. NP_230134; 287 aa, 48% overall identity with an 84% conserved TM3-β domain region). A more distant MscS orthologue is coded by RefSeq accession number NP_232581 (291 aa, 21% identity). An additional ORF predicts a longer 569-aa protein with an N-terminal extension (available at RefSeq under accession no. NP_231387; 37% identity of the homologous C-terminal part to *E. coli* MscS). A putative orthologue of *E. coli* MscM (YbdG) (Schumann et al., 2010) is also present in the N16961 *V. cholerae* genome (available at RefSeq under accession no. NP_229921; 412 aa, 54% identity), but there is no obvious orthologue of MscK (KefA) (Li et al., 2002). Because these channel species have not been characterized individually, we presume that MscS-like activities can potentially be generated by a mixed channel population.

Based on the densities of active channels in excised patches (Table 1), the numbers of channels per cell (5–8 μm^2 in surface area) can be estimated as 18–30 heptameric MscSs and 20–35 pentameric MscLs in AW405 *E. coli*. *V. cholerae*, respectively, should have 6–10 MscS-like and 50–90 functional MscL-like channels per cell. Our estimation of the number of *E. coli* MscL channels is approximately two to three times lower than previously determined in fluorescent microscopy experiments (Bialecka-Fornal et al., 2012), which estimated 300–400 MscL subunits per cell grown in MLB medium. It is possible that not all synthesized subunits form functional pentamers.

The notable difference in mechanoelectrical responses of the two dominant species is that the density of MscL-like channels is approximately three times higher whereas the density of MscS-like channels is about three times lower in *V. cholerae* compared with *E. coli*. Not only is the proportion of MscL to MscS activities different, but the pressure midpoint ratio $p_{0.5}MscS/p_{0.5}MscL$ for the two dominant channel types in *Vibrio* is lower, at 0.48 ± 0.05 versus 0.60 ± 0.05 for *E. coli*. If we take the MscL-like activation midpoint as a reference, the *Vibrio* MscS-like channel activates earlier than its *E. coli* counterpart. In addition, the *Vibrio* MscS-like wave shows no hysteresis during a 1-s triangular ramp, signifying a faster closing rate than that in *E. coli*. MscS-like channels of *Vibrio* exhibit similar rectifying conductance and tension-dependent inactivating behavior as *E. coli* MscS. *Vibrio* MscS-like channels recover from inactivation as fast as *E. coli* MscS does (Akitake et al., 2007; Kamaraju et al., 2011), with a characteristic time of 1.5 s.

Despite *V. cholerae* N16691 having a three times larger overall density of mechanosensitive channels, it is less tolerant to strong downshocks (1,000–1,200 mosmol) compared with *E. coli* AW405. *Vibrio alginolyticus*, for instance, a strictly marine representative of this genus lacking the *mscL* gene, is extremely sensitive to osmotic downshifts, but expression of *E. coli* MscL in this microorganism was shown to dramatically increase its shock tolerance (Nakamaru et al., 1999). High density of MscL channels in *V. cholerae* might compensate for some other traits that make it osmotically vulnerable. The data above allow us to infer the traits to be considered.

In the event of abrupt osmotic shock, the bacterial osmolyte release system will be able to rescue the cell by releasing excess osmolytes faster than hydrostatic

pressure inside the cell reaches the lytic level. In the beginning, osmotic influx of water will stretch the elastic cell wall and the outer membrane. Tension in the inner membrane during osmotic swelling will begin to develop as the membrane unfolds. The kinetics of tension buildup will be defined by the magnitude of the osmotic gradient, elasticity of the cell wall, and the membrane excess area, which requires a certain degree of cell wall distension. Once the threshold tension that activates mechanosensitive channels is reached, the rate of osmolyte release should be high enough to negate the osmotic water influx before critical rupturing tension develops. The observed lower tolerance of *V. cholerae* to abrupt osmotic downshocks compared with *E. coli*, despite a higher density of MscL, points to the necessity of better understanding the following three factors.

(1) Distribution of cell sizes in the population. According to the law of Laplace, tension in the membrane is proportional to the pressure gradient multiplied by the radius of curvature, and thus larger cells must be more vulnerable. It has been well documented that stress conditions lead to the decrease of average size in microbial populations (Barcina, 1995; Chaiyanan et al., 2001). In exponential cultures, *V. cholerae* cells appear to be slightly larger than *E. coli*. The lower tail of size distributions in both populations may constitute the most shock-tolerant cells. In addition to outward cell geometry, the excess amount of membrane, and the mechanical strength of the retaining cell wall (peptidoglycan layer), might vary between the two species.

(2) Water permeability and relative densities of MscS and MscL. Under hydrostatic pressure of water flooding the cytoplasm through the membrane and aquaporins, MscS is predicted to open first and dissipate osmotic gradients. If MscS's osmolyte permeability is insufficient, building up tension will open MscL, a true emergency valve that activates near the lytic tension. Earlier activation of MscS would mediate a more gradual permeability response with tension, which might be beneficial. The density of MscS-like channels in *V. cholerae* under the specific conditions of this study is lower than in *E. coli*; thus, the first line of defense is not as strong. In *E. coli*, expression of both channels is under the control of stress-activated factor RpoS, and overexpression of one partially represses the other. The physiological role of densities of aquaporins, MscS, and MscL channels in both species needs to be better understood. It was proposed that a high density of MscL may increase effective elasticity of the membrane and thus dampen tension through protein expansion (Boucher et al., 2009). In addition, the clustering and distribution of channels between the cylindrical part of the rod-shaped cell and the poles (Romantsov et al., 2010), where curvatures and tensions are different, may influence the hydrostatic pressure at which threshold tension is reached.

(3) The nature of internal osmolytes and channel permeability. The relatively large size of permeation pores in MscS and MscL may ensure that the release kinetics are comparable with the millisecond kinetics of osmotic swelling (Boer et al., 2011). For this reason, efficiency of compatible osmolyte release might be an important factor defining the speed of cellular escape from osmotic rupture. However, permeabilities of MscS or MscL for organic osmolytes have not been studied in detail. Also, the composition of preferred compatible osmolytes used by each of the bacterial species might be different (Schleyer et al., 1993; Pflughoeft et al., 2003). In this investigation, we were able to observe modulating effects of the common compatible osmolyte trehalose on the behavior of both MscS-like and MscL-like channels. Right-shifts of activation curves were accompanied with substantial inactivation of MscS-like channels. Our single-channel recordings suggest that trehalose present in the cytoplasmic compartment does not freely partition into the pore, yet these conductance measurements do not exclude permeation.

In conclusion, the establishment of *V. cholerae* as a system for electrophysiological analysis opens new perspectives for studies of a mechanically activated osmolyte release system and electrogenic transport in this pathogen. The first patch-clamp survey has shown that *V. cholerae* has lower density of MscS-like channels but higher density of MscL-like channels compared with *E. coli*. Both *V. cholerae* channels have gating and conductive properties comparable to their *E. coli* counterparts. This is the first report on WT *V. cholerae*, which shows that compatible osmolytes, especially trehalose, strongly modulate the mechanoelectrical response, shifting activation curves to the right. Trehalose does not seem to partition freely into the open MscL channel, bringing into question the actual exit path of this abundant osmolyte. The comparison of *E. coli* and *V. cholerae*'s sensitivities to osmotic downshock strongly suggests that there must be other factors that contribute to the environmental fitness of this bacterium other than just the density of mechanosensitive channels in its membrane.

The authors thank Claire Costenoble-Caherty for expert technical assistance with bacterial cultures, BLAST searches, and alignments.

This work was partially supported by the National Institutes of Health (NIH; grant RO1 A1039129-11A2) and the National Science Foundation (grant 0813066 to A. Huq and NIH grant R21 AI105655-01 to S. Sukharev and A. Huq).

Edward N. Pugh Jr. served as editor.

Submitted: 4 March 2013
Accepted: 5 June 2013

REFERENCES

Akitake, B., A. Anishkin, and S. Sukharev. 2005. The "dashpot" mechanism of stretch-dependent gating in MscS. *J. Gen. Physiol.* 125:143–154. http://dx.doi.org/10.1085/jgp.200409198

Akitake, B., A. Anishkin, N. Liu, and S. Sukharev. 2007. Straightening and sequential buckling of the pore-lining helices define the gating cycle of MscS. *Nat. Struct. Mol. Biol.* 14:1141–1149. http://dx.doi.org/10.1038/nsmb1341

Anishkin, A., V. Gendel, N.A. Sharifi, C.S. Chiang, L. Shirinian, H.R. Guy, and S. Sukharev. 2003. On the conformation of the COOH-terminal domain of the large mechanosensitive channel MscL. *J. Gen. Physiol.* 121:227–244. http://dx.doi.org/10.1085/jgp.20028768

Anishkin, A., K. Kamaraju, and S. Sukharev. 2008. Mechanosensitive channel MscS in the open state: Modeling of the transition, explicit simulations, and experimental measurements of conductance. *J. Gen. Physiol.* 132:67–83. http://dx.doi.org/10.1085/jgp.200810000

Barcina, I. 1995. Survival strategies of enteric bacteria in aquatic systems. *Microbiologia.* 11:389–392.

Berrier, C., M. Besnard, B. Ajouz, A. Coulombe, and A. Ghazi. 1996. Multiple mechanosensitive ion channels from Escherichia coli, activated at different thresholds of applied pressure. *J. Membr. Biol.* 151:175–187. http://dx.doi.org/10.1007/s002329900068

Bialecka-Fornal, M., H.J. Lee, H.A. DeBerg, C.S. Gandhi, and R. Phillips. 2012. Single-cell census of mechanosensitive channels in living bacteria. *PLoS ONE.* 7:e33077. http://dx.doi.org/10.1371/journal.pone.0033077

Boer, M., A. Anishkin, and S. Sukharev. 2011. Adaptive MscS gating in the osmotic permeability response in E. coli: the question of time. *Biochemistry.* 50:4087–4096. http://dx.doi.org/10.1021/bi1019435

Boucher, P.A., C.E. Morris, and B. Joós. 2009. Mechanosensitive closed-closed transitions in large membrane proteins: osmoprotection and tension damping. *Biophys. J.* 97:2761–2770. http://dx.doi.org/10.1016/j.bpj.2009.08.054

Britten, R.J., and F.T. McClure. 1962. The amino acid pool in Escherichia coli. *Bacteriol. Rev.* 26:292–335.

Chaiyanan, S., S. Chaiyanan, A. Huq, T. Maugel, and R.R. Colwell. 2001. Viability of the nonculturable Vibrio cholerae O1 and O139. *Syst. Appl. Microbiol.* 24:331–341. http://dx.doi.org/10.1078/0723-2020-00032

Chang, G., R.H. Spencer, A.T. Lee, M.T. Barclay, and D.C. Rees. 1998. Structure of the MscL homolog from Mycobacterium tuberculosis: a gated mechanosensitive ion channel. *Science.* 282:2220–2226. http://dx.doi.org/10.1126/science.282.5397.2220

Chiang, C.S., A. Anishkin, and S. Sukharev. 2004. Gating of the large mechanosensitive channel in situ: estimation of the spatial scale of the transition from channel population responses. *Biophys. J.* 86:2846–2861. http://dx.doi.org/10.1016/S0006-3495(04)74337-4

Csonka, L.N., and A.D. Hanson. 1991. Prokaryotic osmoregulation: genetics and physiology. *Annu. Rev. Microbiol.* 45:569–606. http://dx.doi.org/10.1146/annurev.mi.45.100191.003033

Duret, G., and A.H. Delcour. 2006. Deoxycholic acid blocks vibrio cholerae OmpT but not OmpU porin. *J. Biol. Chem.* 281:19899–19905. http://dx.doi.org/10.1074/jbc.M602426200

Duret, G., V. Simonet, and A.H. Delcour. 2007. Modulation of Vibrio cholerae porin function by acidic pH. *Channels (Austin).* 1:70–79.

Grajkowski, W., A. Kubalski, and P. Koprowski. 2005. Surface changes of the mechanosensitive channel MscS upon its activation, inactivation, and closing. *Biophys. J.* 88:3050–3059. http://dx.doi.org/10.1529/biophysj.104.053546

Grim, C.J., N.A. Hasan, E. Taviani, B. Haley, J. Chun, T.S. Brettin, D.C. Bruce, J.C. Detter, C.S. Han, O. Chertkov, et al. 2010. Genome sequence of hybrid Vibrio cholerae O1 MJ-1236, B-33, and CIRS101 and comparative genomics with V. cholerae. *J. Bacteriol.* 192:3524–3533. http://dx.doi.org/10.1128/JB.00040-10

Gullingsrud, J., and K. Schulten. 2003. Gating of MscL studied by steered molecular dynamics. *Biophys. J.* 85:2087–2099. http://dx.doi.org/10.1016/S0006-3495(03)74637-2

Hall, J.E. 1975. Access resistance of a small circular pore. *J. Gen. Physiol.* 66:531–532. http://dx.doi.org/10.1085/jgp.66.4.531

Heidelberg, J.F., J.A. Eisen, W.C. Nelson, R.A. Clayton, M.L. Gwinn, R.J. Dodson, D.H. Haft, E.K. Hickey, J.D. Peterson, L. Umayam, et al. 2000. DNA sequence of both chromosomes of the cholera pathogen Vibrio cholerae. *Nature.* 406:477–483. http://dx.doi.org/10.1038/35020000

Hille, B. 2001. Ionic Channels of Excitable Membranes. Third edition. Sinauer Asssociates, Inc., Sunderland, MA. 814 pp.

Huq, A., and C.J. Grim. 2011. Aquatic realm and cholera. *In* Epidemiological and Molecular Aspects on Cholera (Infectious Disease). T. Ramamurthy and S.K. Bhattachrya, editors. Springer, New York. 311–340.

Kamaraju, K., V. Belyy, I. Rowe, A. Anishkin, and S. Sukharev. 2011. The pathway and spatial scale for MscS inactivation. *J. Gen. Physiol.* 138:49–57. http://dx.doi.org/10.1085/jgp.201110606

Keymer, D.P., M.C. Miller, G.K. Schoolnik, and A.B. Boehm. 2007. Genomic and phenotypic diversity of coastal Vibrio cholerae strains is linked to environmental factors. *Appl. Environ. Microbiol.* 73:3705–3714. http://dx.doi.org/10.1128/AEM.02736-06

Koch, A.L., and S. Woeste. 1992. Elasticity of the sacculus of Escherichia coli. *J. Bacteriol.* 174:4811–4819.

Levina, N., S. Tötemeyer, N.R. Stokes, P. Louis, M.A. Jones, and I.R. Booth. 1999. Protection of Escherichia coli cells against extreme turgor by activation of MscS and MscL mechanosensitive channels: identification of genes required for MscS activity. *EMBO J.* 18:1730–1737. http://dx.doi.org/10.1093/emboj/18.7.1730

Li, Y., P.C. Moe, S. Chandrasekaran, I.R. Booth, and P. Blount. 2002. Ionic regulation of MscK, a mechanosensitive channel from Escherichia coli. *EMBO J.* 21:5323–5330. http://dx.doi.org/10.1093/emboj/cdf537

Luzardo, M.C., F. Amalfa, A.M. Nuñez, S. Díaz, A.C. Biondi De Lopez, and E.A. Disalvo. 2000. Effect of trehalose and sucrose on the hydration and dipole potential of lipid bilayers. *Biophys. J.* 78:2452–2458. http://dx.doi.org/10.1016/S0006-3495(00)76789-0

Martinac, B., M. Buechner, A.H. Delcour, J. Adler, and C. Kung. 1987. Pressure-sensitive ion channel in Escherichia coli. *Proc. Natl. Acad. Sci. USA.* 84:2297–2301. http://dx.doi.org/10.1073/pnas.84.8.2297

Moe, P., and P. Blount. 2005. Assessment of potential stimuli for mechano-dependent gating of MscL: effects of pressure, tension, and lipid headgroups. *Biochemistry.* 44:12239–12244. http://dx.doi.org/10.1021/bi0509649

Moe, P.C., P. Blount, and C. Kung. 1998. Functional and structural conservation in the mechanosensitive channel MscL implicates elements crucial for mechanosensation. *Mol. Microbiol.* 28:583–592. http://dx.doi.org/10.1046/j.1365-2958.1998.00821.x

Naismith, J.H., and I.R. Booth. 2012. Bacterial mechanosensitive channels—MscS: evolution's solution to creating sensitivity in function. *Annu Rev Biophys.* 41:157–177. http://dx.doi.org/10.1146/annurev-biophys-101211-113227

Nakamaru, Y., Y. Takahashi, T. Unemoto, and T. Nakamura. 1999. Mechanosensitive channel functions to alleviate the cell lysis of marine bacterium, Vibrio alginolyticus, by osmotic downshock. *FEBS Lett.* 444:170–172. http://dx.doi.org/10.1016/S0014-5793(99)00054-X

Naughton, L.M., S.L. Blumerman, M. Carlberg, and E.F. Boyd. 2009. Osmoadaptation among Vibrio species and unique genomic features and physiological responses of Vibrio parahaemolyticus. *Appl. Environ. Microbiol.* 75:2802–2810. http://dx.doi.org/10.1128/AEM.01698-08

Pagel, M., and A.H. Delcour. 2011. Effects of conjugated and unconjugated bile acids on the activity of the Vibrio cholerae porin OmpT. *Mol. Membr. Biol.* 28:69–78. http://dx.doi.org/10.3109/09687688.2010.519727

Perozo, E. 2006. Gating prokaryotic mechanosensitive channels. *Nat. Rev. Mol. Cell Biol.* 7:109–119. http://dx.doi.org/10.1038/nrm1833

Pflughoeft, K.J., K. Kierek, and P.I. Watnick. 2003. Role of ectoine in Vibrio cholerae osmoadaptation. *Appl. Environ. Microbiol.* 69:5919–5927. http://dx.doi.org/10.1128/AEM.69.10.5919-5927.2003

Pruzzo, C., A. Huq, R.R. Colwell, and G. Donelli. 2005. Pathogenic *Vibrio* species in the marine and estuarine environment. *In* Oceans and Health: Pathogens in the Marine Environment. R.C. Belkin and R. Colwell, editors. Springer, New York. 217–252.

Romantsov, T., A.R. Battle, J.L. Hendel, B. Martinac, and J.M. Wood. 2010. Protein localization in Escherichia coli cells: comparison of the cytoplasmic membrane proteins ProP, LacY, ProW, AqpZ, MscS, and MscL. *J. Bacteriol.* 192:912–924. http://dx.doi.org/10.1128/JB.00967-09

Rudolph, A.S., J.H. Crowe, and L.M. Crowe. 1986. Effects of three stabilizing agents—proline, betaine, and trehalose—on membrane phospholipids. *Arch. Biochem. Biophys.* 245:134–143. http://dx.doi.org/10.1016/0003-9861(86)90197-9

Ruthe, H.J., and J. Adler. 1985. Fusion of bacterial spheroplasts by electric fields. *Biochim. Biophys. Acta.* 819:105–113. http://dx.doi.org/10.1016/0005-2736(85)90200-7

Schleyer, M., R. Schmid, and E.P. Bakker. 1993. Transient, specific and extremely rapid release of osmolytes from growing cells of Escherichia coli K-12 exposed to hypoosmotic shock. *Arch. Microbiol.* 160:424–431. http://dx.doi.org/10.1007/BF00245302

Schumann, U., M.D. Edwards, T. Rasmussen, W. Bartlett, P. van West, and I.R. Booth. 2010. YbdG in Escherichia coli is a threshold-setting mechanosensitive channel with MscM activity. *Proc. Natl. Acad. Sci. USA.* 107:12664–12669. http://dx.doi.org/10.1073/pnas.1001405107

Steinbacher, S., R. Bass, P. Strop, and D.C. Rees. 2007. Structures of the prokaryotic mechanosensitive channels MscL and MscS. *Curr. Top. Membr.* 58:1–24. http://dx.doi.org/10.1016/S1063-5823(06)58001-9

Stokes, N.R., H.D. Murray, C. Subramaniam, R.L. Gourse, P. Louis, W. Bartlett, S. Miller, and I.R. Booth. 2003. A role for mechanosensitive channels in survival of stationary phase: regulation of channel expression by RpoS. *Proc. Natl. Acad. Sci. USA.* 100:15959–15964. http://dx.doi.org/10.1073/pnas.2536607100

Sukharev, S. 2002. Purification of the small mechanosensitive channel of Escherichia coli (MscS): the subunit structure, conduction, and gating characteristics in liposomes. *Biophys. J.* 83:290–298. http://dx.doi.org/10.1016/S0006-3495(02)75169-2

Sukharev, S.I., B. Martinac, V.Y. Arshavsky, and C. Kung. 1993. Two types of mechanosensitive channels in the Escherichia coli cell envelope: solubilization and functional reconstitution. *Biophys. J.* 65:177–183. http://dx.doi.org/10.1016/S0006-3495(93)81044-0

Sukharev, S.I., W.J. Sigurdson, C. Kung, and F. Sachs. 1999. Energetic and spatial parameters for gating of the bacterial large conductance mechanosensitive channel, MscL. *J. Gen. Physiol.* 113:525–540. http://dx.doi.org/10.1085/jgp.113.4.525

Villarreal, M.A., S.B. Díaz, E.A. Disalvo, and G.G. Montich. 2004. Molecular dynamics simulation study of the interaction of trehalose with lipid membranes. *Langmuir.* 20:7844–7851. http://dx.doi.org/10.1021/la049485l

Wood, J.M., E. Bremer, L.N. Csonka, R. Kraemer, B. Poolman, T. van der Heide, and L.T. Smith. 2001. Osmosensing and osmoregulatory compatible solute accumulation by bacteria. *Comp. Biochem. Physiol. A Mol. Integr. Physiol.* 130:437–460. http://dx.doi.org/10.1016/S1095-6433(01)00442-1